Geophysical Methods for Differentiating Hydrocarbon and Groundwater Signatures: A Narrative Review of Techniques, Diagnostic Criteria and Field Performance

Emmanuel Kobina Gyasi [1], Bernard Nkrumah Attobrah [2], Michael Aziriba Mbah [3], Elvis Sekyere Owusu [3]

[1] *Kansas State University*
919 Mid-Campus Drive North, Manhattan, KS 66506, USA

[2] *New Mexico Institute of Mining and Technology*
801 Leroy Place, Socorro, NM 87801, USA

[3] *Texas Christian University*
Fort Worth, TX 76129, USA

DOI: 10.22178/pos.128-7

LCC Subject Category: T1-995

Received 27.02.2026
Accepted 27.03.2026
Published online 31.03.2026

Corresponding Author:
Emmanuel Kobina Gyasi

Abstract. The petroleum hydrocarbon contamination of shallow aquifers is a continuing problem in site characterisation because the geophysical signatures of hydrocarbon-bearing areas overlap with those of clean groundwater under certain geological and temporal conditions. This narrative review assesses the diagnostic capability of four classes of geophysical methods, electrical resistivity and induced polarisation, electromagnetic (ground penetrating radar, time-domain and frequency-domain electromagnetics), seismic, and combined multi-method methodologies, to distinguish between hydrocarbon and groundwater geophysical signatures at depths of 1-50 m onshore. Scopus, Web of Science, and Google Scholar were synthesised thematically between 2010 and 2025, with pre-2010 sources incorporated because no current substitute exists. Evidence was systematised by method class and evaluated for consistency, geographic coverage, and quality. The most field-proven combination was electrical resistivity imaging together with induced polarisation, but contamination age reverses the resistivity response between resistive and conductive conditions due to biodegradation. Ground penetrating radar eliminated thin layers of LNAPL that the resistivity techniques could not detect, but not where the conductivity of the subsurface was greater than 0.28 S/m. Seismic was used to map the structure rather than to perform outright fluid discrimination at low depths. Researchers obtained the most reliable discrimination results across different site conditions by using staged, multi-method workflows comprising structural characterisation, fluid-sensitive measurements, and geochemical validation. Practitioners examining contaminated sites should use ERT-IP as the primary screening tool, complement it with GPR when vadose-zone conditions are present, and verify the presence of the anomaly through targeted hydrochemical sampling.

Keywords: electrical resistivity tomography; induced polarisation; ground penetrating radar; hydrocarbon contamination; groundwater; LNAPL; geophysical fluid discrimination.

INTRODUCTION

One of the most common forms of groundwater degradation worldwide is petroleum hydrocarbon contamination in shallow aquifers. Groundwater is the source of drinking water for approximately one-third of the global population [1], and petroleum extraction and refining, as well as

storage and transportation, regularly inject light non-aqueous phase liquids (LNAPLs) into the vadose and saturated zones [2]. The amount of crude oil released into the environment annually has been estimated at 0.6 million tonnes [3], and petroleum hydrocarbons are included on regulatory priority lists of pollutants in most jurisdictions because of their mutagenic, carcinogenic, and endocrine-disrupting properties [2, 4]. Precise definition of the boundary between areas influenced by hydrocarbons and uncontaminated groundwater is thus the core of risk assessment and remediation planning; however, traditional methods such as drilling boreholes, soil sampling, and chemical analysis of groundwater provide only point-scale data at high cost and with slow response time [5].

As an alternative to invasive techniques, surface geophysical methods can map subsurface fluid contrasts over lateral distances of hundreds of meters, with vertical resolutions ranging from centimetres (ground-penetrating radar) to meters (electrical resistivity tomography). In the last 30 years, electrical resistivity, induced polarisation, electromagnetic, and seismic methods have been used at hydrocarbon-contaminated sites, producing a substantial but disjointed evidence base. Several intricacies have arisen. New hydrocarbon spills exhibit resistive geophysical signatures similar to those of insulating petroleum fluids. Still, biodegrading contamination can entirely reverse this signature and produce conductive anomalies identical to those of water-saturated clay [6, 7]. Geological environments with a high clay content also make interpretation more difficult because they produce low-resistance responses that are not related to contamination [8]. Geophysical methods measure different physical properties—bulk resistivity, dielectric permittivity, chargeability, and acoustic velocity—and the ability of each property to distinguish hydrocarbons from groundwater depends on the method, contaminant age, and site geology.

Nevertheless, despite the number of published field studies, researchers have not recently synthesised and compared these geophysical techniques by evaluating not only whether each technique recognises contamination but also under what circumstances it can reliably separate hydrocarbon-bearing regions from groundwater-saturated formations. Previous reviews have discussed biogeophysical processes at LNAPL locations [7], the evolution of hydrogeophysics as a tool to characterise the subsurface environment [9], or the attenuation of GPR signals to detect contamination [10], without necessarily comparing diagnostic capabilities among method classes, or how conditions in the field prefer a particular technique over another.

This is a gap in this review. It aims to measure the diagnostic capability of four classes of geophysical methods, including electrical resistivity and induced polarisation, electromagnetic (GPR, TDEM, and FDEM), seismic, and integrated multimethod techniques to discriminate between hydrocarbon and groundwater signatures in onshore shallow subsurface environments. The extent is restricted to surface and near-surface techniques used at depths of 1-50 m, relying mainly on field studies published in recent years (2010-25), with precursors that go deeper, where no recent alternatives are available. Figure 1 represents the diagnostic depth range and site-condition limitations of each method class.

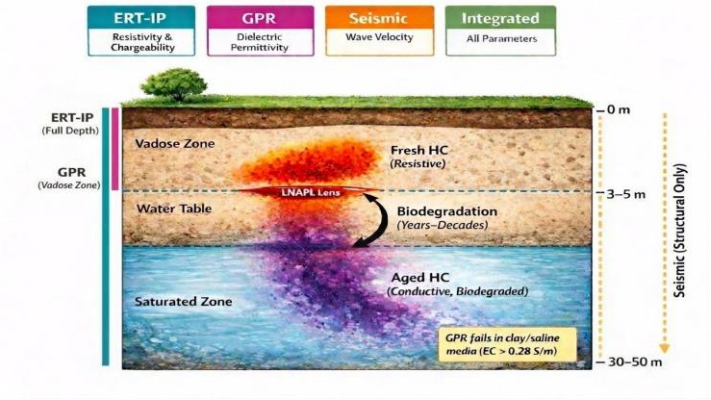

Figure 1 – Geophysical method diagnostic ranges at a contaminated site

METHODS

This narrative review summarised published studies on the use of geophysical techniques to distinguish between hydrocarbon-bearing and groundwater-saturated zones in shallow onshore subsurface environments. No PRISMA accounting, meta-analysis, or systematic review protocol was used.

Between January and March 2026, the researchers performed literature searches in Scopus, Web of Science, Google Scholar, and the U.S. EPA Environmental Geophysics archive. The concept-level search domains were electrical resistivity and hydrocarbon contamination; induced polarisation and fluid discrimination; ground-penetrating

radar and LNAPL detection; electromagnetic methods and groundwater characterisation; seismic methods and pore-fluid identification; and integrated geophysical surveys at contaminated sites. Primary evidence was limited to 20102025 in date but included pre-2010 sources that provided underlying frameworks, namely the biogeophysical model of resistivity evolution at LNAPL reservoirs and the canonical AVO fluid discrimination theory, in both cases for which no recent substitutes exist.

Inclusion criteria were limited to field-based studies that had quantitative geophysical results (resistivity values, chargeability, dielectric permittivity contrasts, seismic velocities, or survey configurations) at sites with known hydrocarbon pollution or known groundwater targets. The researchers included only laboratory studies that provided calibration data directly cited in field studies. Sources were also filtered out when they dealt only with borehole logging without surface-method comparison, marine or offshore contexts, remote sensing with no ground-based geophysical validation, or geochemical-only evaluations with no geophysical elements. The researchers also excluded non-English publications and conference abstracts without full text. Data extraction was based on seven variables: geophysical method and configuration; study design and scale; sample size or survey extent; target depth range; measured physical property values; type and age of contamination; and geological setting. Evidence was sorted by geophysical method of classification, electrical and induced polarisation, electromagnetic, seismic and integrated multi-method and rated narratively to provide consistency of findings, geographic coverage and quality of method used. The researchers did not use a formal tool to assess risk of bias; instead, they assessed evidence quality based on borehole validation, sample size, and the reproducibility of reported measurements at independent sites.

RESULTS AND DISCUSSION

Electrical Resistivity and Induced Polarisation Methods. Electrical resistivity imaging (ERI) is a technique that records the contrast between hydrocarbons and groundwater based on the bulk resistivity of petroleum fluids and formation water. New hydrocarbon contamination always results in high resistivity. Authors [11] measured values of 15,000-60,000 ohms-m in contaminated topsoil at 0.0-3.5m depth around a refinery in Nigeria, an order of magnitude higher than background, with TPH values of 0.342-0.572 mg/L in surrounding groundwater. Another pipeline spill in France in 2009, with 4700 tons of oil released, demonstrated an initial resistive anomaly, measurable across 64 electrodes with 2.5 m separation; a repeat survey three years later recorded resistivity changes in the contaminated zone and stable reference areas [12].

Researchers have observed such temporal changes in conductive and resistive signatures across a variety of hydrogeological environments, and they obtained one of the earliest and most detailed pieces of evidence at the Carson City refinery site in Michigan, which had been contaminated for more than 50 years. Authors [13] used vertical resistivity probes coupled with multilevel piezometers to measure in situ bulk conductivity with a vertical resolution of 5 cm. They observed that at contaminated sites, TDS were 123681 mg/L, whereas at uncontaminated sites, TDS were 50560 mg/L. ERT measurements over two years at a diesel tank leak in Belgium, made above the water table, found resistivities less than 100 m below 10 -1 [14]. Multi-year ERT operations at the Trecate crude oil blow-out site, which had been contaminated since 1994, showed that residual LNAPL areas exhibited conductive rather than resistive signatures, consistent with advanced biodegradation [15]. Table 1 summarises the design, setting, and headline results of the studies reviewed across the four method classes.

Table 1 – Characteristics of key studies reviewed

Study	Methods	Site/Country	Depth	Key Metric	Headline Finding	Notable Limits
[11]	ERI	Refinery, Nigeria	0–3.5 m	Resistivity	15,000–60,000 Ω·m in fresh HC zone	No temporal monitoring
[12]	ERI time-lapse	Pipeline spill, France	0–10 m	Resistivity change	Resistivity decreased over 3 yr in the plume	Single site; no IP
[13]	ERI + probes	Carson City, USA	0–5 m	Bulk conductivity	TDS 123–681 mg/L at contaminated locs	Point measurements
[14]	ERT	Diesel tank,	0–8 m	Resistivity	<10 Ω·m in most	Single

Study	Methods	Site/Country	Depth	Key Metric	Headline Finding	Notable Limits
	monitoring	Belgium			contaminated zones	contaminant type
[15]	ERT + GPR + EMI	Trecate blow-out, Italy	0–15 m	Resistivity, GPR reflections	Aged LNAPL conductive; GPR resolved thin layer	Alluvial setting only
[16]	SIP 0.1–1000 Hz	Carson City, USA	0–5 m	Imaginary conductivity	IP discriminated 3 contamination zones	Lab + field; small N
[8]	TD-IP tomography	Industrial site, Belgium	0–12 m	Chargeability	IP delineated plume better than resistivity	Clay interference
[17]	SIP 0.06–1000 Hz	Hydrogenation plant, Germany	0–10 m	Phase spectra	Resolved source + dissolved plume	Complex site history
[18]	GPR 100–500 MHz	Sand pit + spill, USA	0–3 m	Dielectric contrast	Clear LNAPL anomaly in clean sand	Controlled conditions
[19]	GPR + VES	Landfill, Brazil	0–5 m	GPR penetration	GPR failed in clay interbeds	Single site
[20]	TDEM + geochem	Coastal aquifer, Tunisia	0–80 m	Resistivity + ion ratios	Brine vs seawater discriminated	No LNAPL target
[21]	AVO	Kadanwari field, Pakistan	1,500–2,500 m	Intercept, fluid factor	Gas vs brine separated by AVO	Reservoir depth only
[22]	Shallow seismic	Sand column, USA (lab)	0–2 m	Vp, Vp/Vs	Vp <1,500 m/s = incomplete saturation	Lab scale; no field HC
[23]	ERT + IP + GPR + SP	Aged plume, France	0–15 m	4 independent parameters	All 4 signatures converged on the plume	Single-aged site
[5]	VES + 2D/3D ERT + geochem	Oil spill, Niger Delta	0–24+ m	Resistivity + TPH	TPH 722.75 μg/L; 2 aquifers invaded	No IP data
[24]	Seis + GPR + ERT + IP	Clay-rich site, South Korea	0–15 m	Staged workflow	The staged approach corrected misclassification	Limited borehole count

Induced polarisation (IP) provides a second diagnostic parameter, chargeability, that responds to electrochemical processes at grain-fluid interfaces. IP measurements at 0.1–1,000 Hz on Carson City sediments showed that imaginary conductivity discriminated three contamination zones: smear zone samples produced the highest values, followed by dissolved-phase zones, and then uncontaminated background [16]. Real conductivity did not correlate with contamination status, whereas the IP component separated all three zones. Time-domain IP tomography at an industrial site in Belgium delineated contaminated volumes more precisely than resistivity alone, particularly where clay variability confounded resistivity interpretation [8]. Spectral IP deployed across 0.06–1,000 Hz at a former hydrogenation plant in Germany resolved both source-zone and dissolved-plume geometries that resistivity surveys alone could not distinguish [17]. Field IP surveys over an olive oil mill waste site in Crete, Greece, further confirmed that the polarizability anomaly tracked contamination extent more closely than the conductivity image, which reflected background hydrogeological variability [25].

Electromagnetic Methods. Ground-penetrating radar (GPR) is a technique that identifies hydrocarbon-groundwater boundaries in variations in dielectric permittivity, which is a measure of the speed of electromagnetic waves and their ability to bounce back. The relative permittivity of water is about 80, whereas most petroleum NAPLs range from 2 to 10; this difference leads to strong reflections when pore water is replaced by hydrocarbons [26]. Experiments at Ohio State University with controlled sandpits showed that GPR is sensitive to LNAPL at 100500 MHz when using an antenna at 100500 MHz over a container of diesel-saturated sand [18]. Repeat surveys at a gasoline spill site in Indiana during the winter season indicated that data collected on partially frozen ground are more sensitive to the presence of gasoline in winter than those collected during summer, because low moisture in the unsaturated zone displaced the dielectric contrasts in the contaminated site [18].

Old contamination has another GPR response. Authors [27] reported attenuated GPR reflections, termed shadow zones, at the same Michigan refinery where the resistivity reversibility was observed, rather than the amplified reflections expected from a resistive hydrocarbon layer. At the Trecate site, GPR data identified a strong near-surface reflector, which researchers interpreted as residual free-phase hydrocarbon in the vadose zone, and which co-located with ERT measurements that could not resolve the layer due to its limited thickness [15]. At standard survey frequencies (200 400 MHz), the vertical resolution of GPR can be 5 15 cm in dry sand, and LNAPL lenses thinner than the resolution limit of electrode-based systems can be detected [26].

GPR has limited applications due to depth penetration. Conductive media attenuate signals quickly, so the effective survey depth is less than 5 m in clay-based soils and less than 112 m in salty or wet conditions [28]. In southeastern Brazil, a landfill survey effectively mapped the contamination plume boundary in sandy sediments, but lacked resolution in areas with preponderant clay interbeds [19]. The analysis of a model corroborated that the amplitude of the reflected wave would tend to zero when the electrical conductivity of the subsurface exceeded 0.28 S/m, which is the numerical limit of GPR application in conductive environments [29].

Time-domain electromagnetic (TDEM) techniques can reach deeper depths (usually 50250 m) but respond primarily to conductive targets [30]. TDEM surveys are effective in mapping saline groundwater: 28 soundings in the coastal region of Oman identified the fresh water-salty boundary of an alluvial aquifer [31], and TDEM pseudosections with geochemical tracers in the coastal plain of the Wadi Al Ayn in Tunisia identified the infiltration of oilfield brine with seawater intrusion [20]. To distinguish between resistive LNAPL accumulations and adjacent formations, TDEM is not as sensitive as GPR and ERI at shallow depths, and there are no published field applications that have used TDEM to identify LNAPL with adequate confidence.

Frequency-domain electromagnetic (FDEM) tools offer high-speed lateral conductivity mapping at shallow depths (typically 36 m). In Carson City, FDEM surveying did not detect the free-product plume at depth, as expected given the method's low vertical resolution and the inability to isolate thin resistive zones in a conductive background [27].

Seismic Methods. Seismic methods measure fluid differences by measuring the effects of compressional (P-wave) and shear (S-wave) wave speeds. The amplitude variation with offset (AVO) analysis has been widely used at reservoir depths to distinguish between oil- and water-saturated zones. In the Kadanwari field in Pakistan, gas sand and brine sand responded to the AVO-derived intercept and fluid factors, which had not previously been used to prevent dry wells using conventional reflection data [21]. A Geostack method applied to a 3-D dataset revealed that fluid factor traces produced excellent amplitude anomalies, limited to the recognised oil field [32]. An AVO equation derived from rock physics enhanced gas separation in tight sandstones, where standard elastic parameters are less sensitive [33].

These methods include high-fold gathers, well log calibration, and processing infrastructure aimed at targets hundreds to thousands of meters deep. Near-surface seismic surveys are affected by source-generated noise, guided waves, and surface wave interference that are dominant at shallow offset frequencies [34]. Velocity contrasts generated by LNAPL in unconsolidated shallow sediments are smaller and more spatially heterogeneous than those generated in consolidated reservoir rock, further reducing the available signal.

Shallow seismic techniques aid in velocity-based stratigraphic mapping. At the water table, the velocity of p-waves rises suddenly, as in unsaturated sand (0.4-0.8 m/s) with saturated sediments (1,100-1,800 m/s) [35, 36]. Experiments with controlled sand showed that P-wave velocities below 1,500 m/s indicate a lack of saturation [22]. A possible discriminator is the Vp/Vs ratio: in unconsolidated sands, saturated zones would have values in the 3-4 range, whereas unsaturated zones would have values greater than 1.525 [22, 35]. In the Nylsvley Nature Reserve of South Africa, a high-resolution survey was able to map the water table at a depth of 3-5m in alluvial deposits by comparing changes in velocity with simultaneous measurements of resistivity [37].

There is no reliable scientific evidence in the literature indicating seismic differentiation between LNAPL and clean groundwater under shallow, unconsolidated conditions [31]. At contaminated sites where seismic data have been collect-

ed, the contribution has been structural: mapping bedrock topography, fault zones, and stratigraphic boundaries that govern contaminant migration pathways [38].

Integrated Multi-Method Approaches. Single-method geophysical surveys yield non-unique results at hydrocarbon-contaminated sites, prompting the adoption of multi-method approaches. Researchers conducted a prototype study at the heavily instrumented Michigan refinery and demonstrated that resistivity most effectively determined the geometry of contamination, GPR identified attenuated reflection zones in the same locations as the plume, and FDEM did not detect the free-product layer [27]. Later, multi-method campaigns perfected this method.

The Trecate site was a time-lapse platform that combined GPR, ERT, and electromagnetic induction. GPR identified the thin, residual free-phase layer in the vadose zone that ERT could not correct; ERT identified a deeper conductive anomaly in the saturated zone beyond the GPR penetration depth. These two techniques would not have been sufficient to build the complete contamination geometry [15]. The deployment of a four-method deployment (ERT, time-domain IP, GPR and self-potential) at an ancient hydrocarbon plume in France discovered that low-resistivity anomalies accompanied high-chargeability values, attenuated GPR reflections and negative SP anomalies, four independent signatures, which all coincided in the same contaminated zone [23].

Discrimination was enhanced by geochemical validation whenever various conductive sources cooccurred. The TDEM pseudosections in the coastal aquifer of Tunisia did not distinguish between oilfield brine (mixing fraction 1-13) and intruded seawater (mixing fraction 2-21) in the absence of ionic and isotopic tracers [20]. The geophysical anomalies were confirmed through VES, 2D ERT, and 3D ERT surveys, with TPH, PAH, and BTEX analyses in the Niger Delta, where contamination extended to 24 m in depth and had an average TPH concentration of 722.75 μg/L [5]. A 2024 survey of a clay-rich LNAPL site in South Korea used sequentially seismic refraction, GPR, ERT, and IP: structural-independent methods were used first, followed by fluid-sensitive methods that had to be consistent with the structural model. Boreholes also confirmed that this staged methodology had accurately identified the contaminated volumes, whereas single-method ERT had inaccurately identified them as clay [24].

A comparison of four methods reveals that diagnostic ability in hydrocarbon-groundwater discrimination differs significantly across methods, site characteristics, and contamination history. The most robust evidence base and the most diversified applications across fields are associated with electrical resistivity and induced polarisation. At contamination sites, seismic techniques, which are well established at reservoir depths, have not been tested to distinguish near-surface fluids [21, 32, 34]. GPR works well in resistive, sandy, vadose environments but becomes ineffective in conductive, clay-filled, or waterlogged environments, where contamination measurement is most frequently required [19, 26, 29]. No geophysical parameter consistently distinguishes between hydrocarbons and groundwater at every site; site geology, contamination age, and the physical properties themselves equally determine method selection.

The most consequential complication of field interpretation is the resistive-to-conductive transition at LNAPL sites. New contamination increases bulk resistivity by an order of magnitude, to four times the background level, consistent with the Archie law, as petroleum fluids have electrical conductivities orders of magnitude lower than those of typical formation water [11, 12]. Biodegradation undoes this signature in at least three ways: microbial hydrocarbon metabolism forms organic acids and carbonic acid which dissolve minerals in the aquifer and release ionic species to pore water; sulfate-reducing bacteria form hydrogen sulfide which precipitates on surfaces of the grains as conductive metallic sulfides; biosurfactants synthesised during aerobic degrad Field evidence French [12], Michigan [13], Belgium [14] and Italian [15] studies indicate that the transition timescale lies between years to decades and varies with type of contaminant, community structure of microbes and aquifer geochemistry. A single resistivity survey with no information about the history of contamination, thus, cannot be used to identify whether a conductive anomaly is due to water-saturated clay or a biodegraded plume. This non-uniqueness constrains the diagnostic value of resistivity imaging independently at sites of unknown history.

Introducing chargeability as a second independent parameter in IP measurements partly resolves the ambiguity. There are three different

polarisation processes at contaminated sites: membrane polarisation in clay minerals, electrode polarisation of metallic sulfide grain coats formed by biogenic sulfate reduction, and electrochemical polarisation at the biofilm-mineral interface, where biogenic extracellular polymeric substances alter charge-transfer kinetics [7, 16]. The contribution of each mechanism depends on the age of contamination. In sites recently contaminated with limited biodegradation, the IP response is dominated by membrane polarisation in the host clay, making discrimination difficult. Electrode polarisation due to biogenic sulfides is chargeable at aged sites where sulfate reduction occurs, and polarisation increases with the strength of biodegradation, which is the opposite of clay-induced polarisation and thus diagnostic when used together with resistivity data [16]. Data obtained in Carson City field and laboratory demonstrated that imaginary conductivity distinguished contamination zones where real conductivity could not [16], and later work in Belgium, Germany, and Greece established that combined ERT-IP surveys better define contaminated volumes than resistivity alone [8, 17, 25]. It is not yet easily practicable to separate clay-induced and biodegradation-induced chargeability. Still, it requires sufficiently fine electrode separations to measure plume geometry and to calibrate boreholes at complex locations [8].

GPR works on a slim but lucrative scale. The fact that it has never worked in clay terrains and that it can only be useful below the water table in conductive aquifers is attributed to its 0.28 S/m conductivity ceiling [29]. Under suitable conditions, shallow, dry, sandy vadose zones, GPR can identify thin LNAPL lenses at centimetre-scale resolution that ERT cannot [15, 26]. The qualitative diagnostic indicator of the shadow zone response at aged sites [27] should be compared with baseline or reference-area data to differentiate between attenuation caused by biodegradation and lithological loss of signal. This complementary nature of GPR (thin vadose zone objectives, qualitative attenuation mapping) and ERT-IP (deeper saturated zone characterisation, quantitative property contrasts) underpins the integrated workflow observed in recent fieldwork [15, 23, 27].

At fluid reservoir depths, where consolidated rock can generate significant velocity differences between gas, oil, and brine, fluid discrimination, AVO analysis, and Vp/Vs ratios strongly support the identification of different fluids [21, 33]. At depths of 1.30 m of interest for contamination measurement, the velocity differences between LNAPL and groundwater in unconsolidated sediments are minute, spatially irregular, and obscured by noise from sources [22, 34]. Because unconsolidated sands have a low shear modulus, the situation worsens: Vp/Vs ratios respond strongly to even minor changes in saturation near the water table, and analysts can easily misinterpret anomalies unrelated to contamination unless independent validation data are available. The lack of published field evidence of reliable seismic LNAPL discrimination in shallow environments, despite decades of practice, indicates a real physical constraint rather than an understudied research community. At contaminated locations, seismic techniques play the most significant role through structural mapping, which limits the geological framework on which further fluid-sensitive surveys are to be conducted [24, 37, 38].

Staged multi-method deployments that included borehole validation were the most successful at discrimination [5, 15, 23, 24, 27]. The new workflow orders the structural methods (seismic refraction to get topography of the bedrock and the geometry of the layers and GPR to get shallow stratigraphic detail), the fluid-sensitive methods (ERT-IP constrained by the structural model to minimise ambiguity between lithological and contamination responses) and the geochemical sampling (targeting the anomalies observed by geophysics to determine the nature of the fluid This order minimised misclassification compared to any single method survey. The choice of deployment is determined by cost and logistics: ERT-IP needs only small equipment, and can survey hectare areas in a few days, whereas adding seismic refraction doubles field time and processing effort, which is a trade-off that is justified primarily at geologically complex sites where the ambiguity of clay contamination is severe [24]. Geochemical validation was essential in situations with multiple sources of conductive fluid: TDEM could not distinguish between oilfield brine and seawater in a Tunisian coastal aquifer without the aid of ionic and isotopic tracers [20]. Geophysical surveys in hydrocarbon-contaminated areas are spatial screening tools that require geochemical ground truth rather than fluid identification tools per se. Figure 2 depicts the three-phase implementation cycle that arises from these studies.

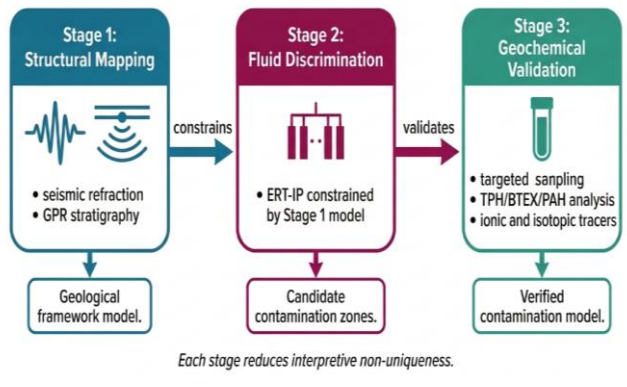

Figure 2 – Three-phase implementation cycle

Several factors limit these conclusions. Geographical focus of the literature is on Nigeria, the United States, and western Europe, but there is little coverage of the Middle East, Central Asia, and south America, where different geological conditions (e.g., arid sabkha formations, lateritic soils, permafrost-affected sediments) and climatic regimes can modify geophysical responses in other ways that are not reflected in the existing evidence base. This geographic bias implies that the resistivity intervals, chargeability, and GPR penetration depths obtained in this study may not be directly applicable to other sites with varying mineralogy, pore-water salinity, or soil moisture regimes.

The bulk of aged-contamination field research is based on a few, heavily monitored reference sites; Carson City and Trecate make a disproportionate contribution to the multi-method, time-series monitoring evidence. They both occur in temperate climates in sandy alluvial aquifers, and the biogeophysical relationships reported at these locations may not be relevant in fractured crystalline rocks, carbonate karst, or tropical laterite environments, where mineral surface chemistry varies significantly.

Publication bias is likely to favour positive detection results, underrepresenting surveys with ambiguous or null results at confirmed contamination sites. The practical implication here is that the success rates of the methods reported in the literature will be exaggerated relative to the reliability practitioners can anticipate in normal site testing.

There is limited data on temporal monitoring. In the majority of studies, single-survey snapshots are reported rather than repeated measures of the resistive-to-conductive transition at a given location. Researchers poorly constrain the timescale and predictability of signature reversal in most contaminant–aquifer systems when time-series data do not span the entire biodegradation cycle.

The language limit on publications in English might have omitted pertinent field results from the Russian, Chinese, and Latin American oil geophysics communities, where petroleum geophysics courses are operational but publications are in non-English journals.

CONCLUSIONS

Electrical resistivity imaging in conjunction with induced polarisation is the most field-tested method for identifying zones between hydrocarbon-impacted formations and groundwater-saturated ground formations. However, diagnostic accuracy is influenced by the age of contamination and the site's lithology. Ground-penetrating radar can detect thin layers in low-conductivity environments, but not in clay-rich or waterlogged environments. The role of seismic techniques is to provide a structural background, but not to directly indicate fluids in superficial contamination areas. The most discriminative results recorded in the literature were those associated with a staged multi-method survey, structural mapping first, fluid-sensitive measurements second, and geochemical validation third. Assessment practitioners for sites with unclear contamination histories are advised to use ERT-IP as the initial screening tool, with GPR, where feasible, in vadose zones, and with specific hydrochemical sampling to verify geophysical anomalies before investing in remediation designs.

REFERENCES

1. Li, P., Karunanidhi, D., Subramani, T., & Srinivasamoorthy, K. (2021). Sources and consequences of groundwater contamination. *Archives of Environmental Contamination and Toxicology, 80*(1), 1–10. doi: 10.1007/s00244-020-00805-z

2. Kuppusamy, S., Maddela, N. R., Megharaj, M., & Venkateswarlu, K. (2020). *Total Petroleum Hydrocarbons: Environmental Fate, Toxicity, and Remediation.* Springer.

3. Kvenvolden, K. A., & Cooper, C. K. (2003). Natural seepage of crude oil into the marine environment. *Geo-Marine Letters, 23*(3–4), 140–146. doi: 10.1007/s00367-003-0135-0

4. Gaur, V. K., Sharma, P., Sirohi, R., Awasthi, M. K., Dussap, C., & Pandey, A. (2020). Assessing the impact of industrial waste on the environment and mitigation strategies: A comprehensive review. *Journal of Hazardous Materials, 398,* 123019. doi: 10.1016/j.jhazmat.2020.123019

5. Eze, S. U., Ogagarue, D. O., Nnorom, S. L., Osung, W. E., & Ibitoye, T. A. (2021). Integrated geophysical and geochemical methods for environmental assessment of subsurface hydrocarbon contamination. *Environmental Monitoring and Assessment, 193*(7), 451. doi: 10.1007/s10661-021-09219-3

6. Sauck, W. A., Atekwana, E. A., & Nash, M. S. (1998). High Conductivities Associated With an LNAPL Plume Imaged by Integrated Geophysical Techniques. *Journal of Environmental and Engineering Geophysics, 2*(3), 203–212.

7. Atekwana, E. A., & Atekwana, E. A. (2009). Geophysical signatures of microbial activity at hydrocarbon contaminated sites: a review. *Surveys in Geophysics, 31*(2), 247–283. doi: 10.1007/s10712-009-9089-8

8. Deceuster, J., & Kaufmann, O. (2012). Improving the delineation of hydrocarbon-impacted soils and water through induced polarisation (IP) tomographies: A field study at an industrial waste land. *Journal of Contaminant Hydrology, 136*, 25–42. doi: 10.1016/j.jconhyd.2012.05.003

9. Binley, A., Hubbard, S. S., Huisman, J. A., Revil, A., Robinson, D. A., Singha, K., & Slater, L. D. (2015). The emergence of hydrogeophysics for improved understanding of subsurface processes over multiple scales. *Water Resources Research, 51*(6), 3837–3866. doi: 10.1002/2015wr017016

10. Cassidy, N. J. (2007). Evaluating LNAPL contamination using GPR signal attenuation analysis and dielectric property measurements: Practical implications for hydrological studies. *Journal of Contaminant Hydrology, 94*(1–2), 49–75. doi: 10.1016/j.jconhyd.2007.05.002

11. Alao, J. O., Balarabe, B., Ayejoto, D. A., Abubakar, F., Otorkpa, O. J., & Eze, S. U. (2025). Evaluation of hydrocarbon and co-contaminants in groundwater and associated public health risks using electrical resistivity and hydrochemical data. *Water Resources and Industry, 34*, 100319. doi: 10.1016/j.wri.2025.100319

12. Blondel, A., Schmutz, M., Franceschi, M., Tichané, F., & Carles, M. (2014). Temporal evolution of the geoelectrical response on a hydrocarbon-contaminated site. *Journal of Applied Geophysics, 103,* 161–171. doi: 10.1016/j.jappgeo.2014.01.013

13. Atekwana, E. A., Atekwana, E. A., Rowe, R. S., Werkema, D. D., & Legall, F. D. (2004). The relationship of total dissolved solids measurements to bulk electrical conductivity in an aquifer contaminated with hydrocarbons. *Journal of Applied Geophysics, 56*(4), 281–294. doi: 10.1016/j.jappgeo.2004.08.003

14. Caterina, D., Orozco, A. F., & Nguyen, F. (2017). Long-term ERT monitoring of biogeochemical changes of an aged hydrocarbon contamination. *Journal of Contaminant Hydrology, 201*, 19–29. doi: 10.1016/j.jconhyd.2017.04.003

15. Cassiani, G., Binley, A., Kemna, A., Wehrer, M., Orozco, A. F., Deiana, R., Boaga, J., Rossi, M., Dietrich, P., Werban, U., Zschornack, L., Godio, A., JafarGandomi, A., & Deidda, G. P. (2014). Noninvasive characterisation of the Trecate (Italy) crude-oil-contaminated site: links between contamination and geophysical signals. *Environmental Science and Pollution Research, 21*(15), 8914–8931. doi: 10.1007/s11356-014-2494-7

16. Aal, G. Z. A., Slater, L. D., & Atekwana, E. A. (2006). Induced-polarisation measurements on unconsolidated sediments from a site of active hydrocarbon biodegradation. *Geophysics, 71*(2), H13–H24. doi: 10.1190/1.2187760

17. Orozco, A. F., Kemna, A., Oberdörster, C., Zschornack, L., Leven, C., Dietrich, P., & Weiss, H. (2012). Delineation of subsurface hydrocarbon contamination at a former hydrogenation plant using spectral induced polarisation imaging. *Journal of Contaminant Hydrology, 136*, 131–144. doi: 10.1016/j.jconhyd.2012.06.001

18. Daniels, J. J., Roberts, R., & Vendl, M. (1995). Ground penetrating radar for the detection of liquid contaminants. *Journal of Applied Geophysics, 33*(1–3), 195–207. doi: 10.1016/0926-9851(95)90041-1

19. Porsani, J. L., Filho, W. M., Elis, V. R., Shimeles, F., Dourado, J. C., & Moura, H. P. (2004). The use of GPR and VES in delineating a contamination plume in a landfill site: a case study in SE Brazil. *Journal of Applied Geophysics, 55*(3–4), 199–209. doi: 10.1016/j.jappgeo.2003.11.001

20. Chekirbane, A., Tsujimura, M., Kawachi, A., Lachaal, F., Isoda, H., & Tarhouni, J. (2014). Use of a time-domain electromagnetic method with geochemical tracers to explore the salinity anomalies in a small coastal aquifer in north-eastern Tunisia. *Hydrogeology Journal, 22*(8), 1777–1794. doi: 10.1007/s10040-014-1180-7

21. Li, J. (2012). Gas reservoir identification by seismic AVO attributes on fluid substitution. *Applied Geophysics, 9*(2), 139–148. doi: 10.1007/s11770-012-0323-7

22. Bachrach, R., & Nur, A. (1998). High-resolution of shallow-seismic experiments in sand; Part 1, Water table, fluid flow, and saturation. *Geophysics, 63*(4), 1225–1233. doi: 10.1190/1.1444423

23. Abbas, M., Jardani, A., Machour, N., & Dupont, J. (2017). Geophysical and geochemical characterisation of a site impacted by hydrocarbon contamination undergoing biodegradation. *Near Surface Geophysics, 16*(2), 176–192. doi: 10.3997/1873-0604.2017061

24. Kim, B., Joung, I. S., Yu, H., Jeong, J., Song, S. Y., Son, J., Yu, Y., Shin, J., Jo, H. Y., Kwon, M. J., & Nam, M. J. (2023). Delineation of LNAPL plumes in a clay-rich site in Gyeongsangnam-do Province, South Korea: integration of geophysical survey data with borehole data and soil sampling information. *Environmental Monitoring and Assessment, 196*(1), 47. doi: 10.1007/s10661-023-12202-9

25. Ntarlagiannis, D., Robinson, J., Soupios, P., & Slater, L. (2016). Field-scale electrical geophysics over an olive oil mill waste deposition site: Evaluating the information content of resistivity versus induced polarisation (IP) images for delineating the spatial extent of organic contamination. *Journal of Applied Geophysics, 135*, 418–426. doi: 10.1016/j.jappgeo.2016.01.017

26. Reynolds, J. M. (2011). *An Introduction to Applied and Environmental Geophysics* (2nd ed.). John Wiley & Sons.

27. Atekwana, E. A., Sauck, W. A., & Werkema, D. D. (2000). Investigations of geoelectrical signatures at a hydrocarbon contaminated site. *Journal of Applied Geophysics, 44*(2–3), 167–180. doi: 10.1016/s0926-9851(98)00033-0

28. Annan, A. P. (2005). GPR methods for hydrogeological studies. In *Water Science and Technology Library* (pp. 185–213). doi: 10.1007/1-4020-3102-5_7

29. Wijewardana, Y. N. S., Shilpadi, A. T., Mowjood, M. I. M., Kawamoto, K., & Galagedara, L. W. (2017). Ground-penetrating radar (GPR) responses for sub-surface salt contamination and solid waste: modelling and controlled lysimeter studies. *Environmental Monitoring and Assessment, 189*(2), 57. doi: 10.1007/s10661-017-5770-4

30. McNeill, J.D. (1994) Principles and Application of Time Domain Electromagnetic Techniques for Resistivity Sounding. *Technical Note TN-27, Geonics Ltd.*

31. El-Kaliouby, H., & Abdalla, O. (2015). Application of time-domain electromagnetic method in mapping saltwater intrusion of a coastal alluvial aquifer, North Oman. *Journal of Applied Geophysics, 115*, 59–64. doi: 10.1016/j.jappgeo.2015.02.003

32. Fatti, J. L., Smith, G. C., Vail, P. J., Strauss, P. J., & Levitt, P. R. (1994). Detection of gas in sandstone reservoirs using AVO analysis: a 3-D seismic case history using the Geostack technique. *Geophysics, 59*(9), 1362–1376. doi: 10.1190/1.1443695

33. Jin, H., Liu, C., & Guo, Z. (2024). Gas prediction in tight sandstones based on the rock-physics-derived seismic amplitude variation versus offset method. *Petroleum Science, 21*(6), 3951–3964. doi: 10.1016/j.petsci.2024.06.006

34. Steeples, D. W. (2005). Shallow seismic methods. In *Water Science and Technology Library* (pp. 215–251). doi: 10.1007/1-4020-3102-5_8

35. Haines, S. S., & Ellefsen, K. J. (2010). Shear-wave seismic reflection studies of unconsolidated sediments in the near surface. *Geophysics, 75*(2), 59–66. doi: 10.1190/1.3340969

36. Haeni, F. P. (1986). Application of seismic refraction methods in groundwater modelling studies in New England. *Geophysics, 51*(2), 236–249. doi: 10.1190/1.1442083

37. Onyebueke, E. O., Manzi, M. S. D., & Durrheim, R. J. (2018). High-resolution shallow reflection seismic integrated with other geophysical methods for hydrogeological prospecting in the Nylsvley Nature Reserve, South Africa. *Journal of Geophysics and Engineering, 15*(6), 2658–2673. doi: 10.1088/1742-2140/aadbe3

38. Cunningham, K. J. (2013). Integrating seismic-reflection and sequence-stratigraphic methods to characterise the hydrogeology of the Floridan aquifer system in southeast Florida. *Antarctica is a Keystone in a Changing World*. doi: 10.3133/ofr20131181